

Nanometer-scale phase separation in mixed composition self-assembled monolayers

S J Stranick^{†||¶}, S V Atre[‡], A N Parikh^{†+}, M C Wood^{†*},
D L Allara[§], N Winograd[†] and P S Weiss^{†#}

[†] Department of Chemistry, The Pennsylvania State University, University Park, PA 16802, USA

[‡] Department of Materials Science and Engineering, The Pennsylvania State University, University Park, PA 16802, USA

[§] Departments of Chemistry and Materials Science and Engineering, The Pennsylvania State University, University Park, PA 16802, USA

Abstract. Mixed composition monolayers of similar *n*-alkanethiols on Au{111} are formed by self-assembly. While the average surface composition of these films accurately reflects the composition of the deposition solution, scanning tunneling microscopy and secondary ion mass spectroscopy measurements show that the films phase separate on the nanometer scale. Scanning tunneling microscopy has been used to follow molecular motions within these films. We discuss our observations in terms of the formation and stability of the phase-segregated domains, and their potential importance in nanoscale applications.

1. Introduction

As the applications of alloys and composite materials extend into the realm of nanotechnology, an understanding of the properties and behavior of these materials on the molecular scale will become of paramount importance. Critical aspects of these materials are the determination of the nanometer-scale structures formed from multicomponent films and the extent to which these structures can be controlled and stabilized. Here we address the issue of phase separation in mixed composition systems. To this end, we have studied two component quasi-two-dimensional self-assembled monolayers (SAMs) of *n*-alkanethiols on Au{111}.

Densely packed, crystalline SAMs of *n*-alkanethiols on Au{111} spontaneously form when a Au{111} surface is immersed in a solution containing *n*-alkanethiols [1]. These quasi-two-dimensional organic monolayer films are formed by covalently bonding the thiol S to the Au surface, while the alkyl chains interact through van der Waals forces to form an ordered overlayer. The terminal functional groups of the alkyl chains define the exposed surface of

this self-assembled organic layer [1,2]. By varying the functionality of these end groups, the physicochemical nature of the surface can also be varied. It is shown below how the terminal functional groups used in this study, $-\text{CH}_3$, $-\text{CO}_2\text{CH}_3$, $-\text{OH}$, and $-\text{CN}$, determine the structural properties and phase behavior of this system. The *n*-alkanethiols used— $\text{CH}_3(\text{CH}_2)_{15}\text{SH}$, $\text{CH}_3\text{O}_2\text{C}(\text{CH}_2)_{15}\text{SH}$, $\text{HOCH}_2(\text{CH}_2)_{15}\text{SH}$, and $\text{NCCH}_2(\text{CH}_2)_{15}\text{SH}$ —have nearly identical chain lengths and differ only in their terminal functional groups. These slight variations result in the formation and growth of phase-segregated nanometer-scale molecular domains.

Direct observation of phase segregation in Langmuir films by techniques other than the scanning probe microscopies have previously been limited to macroscopic domains [3]. Meyer and co-workers have used frictional force microscopy to study phase segregation in Langmuir–Blodgett films in which two very different component molecules are co-deposited [4,5]. In a series of experiments they have shown how the domain shapes in these relatively mobile films (prior to deposition) depend on alkyl chain length of one of the components [5]. More recently, Lieber and others have used functionalized force microscope probe tips to obtain contrast on patterned SAMs on the micron scale [6]. We have used scanning tunneling microscopy (STM) to demonstrate phase segregation at the molecular scale in varied composition, two-component SAMs [7,8]. The spatial distribution of the molecules comprising the phase-separated domains as well as the temporal evolution of these structures were observed [7]. The formation and

^{||} E-mail address: stm@psu.edu

[¶] Present address: Chemistry Sciences & Technology Laboratory, Surface & Microanalysis Science Division, National Institute of Standards and Technology, Gaithersburg, MD 20899, USA.

⁺ Present address: Materials Science Laboratory, Los Alamos National Laboratory, Los Alamos, NM 87545, USA.

^{*} Present address: Device Microanalysis Center, United States Army Research Laboratory, Fort Monmouth, NJ 07703, USA.

[#] To whom correspondence should be addressed.

growth of these domains has been observed in time-lapse STM imaging [9].

In a recent theoretical experimental treatment of molecular phase segregation in mixed composition SAMs of $\text{CH}_3(\text{CH}_2)_{11}\text{SH}$ and $\text{CH}_3(\text{CH}_2)_{21}\text{SH}$, Folkers *et al* concluded that, in general, a SAM in equilibrium with the deposition solution will be comprised of a single phase of either a pure thiol or a heterogeneous mixture of the two thiols [10]. Folkers *et al* also pointed out that if an exchange between the film and the solution is incomplete (i.e. the sample is removed from solution before equilibrium is reached), then the film may form phase-separated islands [10]. This is certainly the situation in our sample preparation. While the length of time that our samples remain in the solution are an order of magnitude longer than typical immersion times, results of imaging time-of-flight secondary ion mass spectroscopy (TOF-SIMS) studies have shown that the rates of exchange between the solution and the monolayer film are extremely slow at room temperature [11]. In these studies partial and complete monolayers have been immersed in solutions of different thiols and then the films have been analyzed using SIMS. Only in the case where thiols from the initial exposure were not on the surface (e.g. where they had been mechanically removed), were the thiol species from the second exposure found in abundance [11]. Folkers *et al* [10] raised the deposition solution temperature to 60 °C to accelerate SAM-solution exchange in order to attempt to reach equilibrium, but could not ascertain whether they had done so. In recent experiments, we have gone to higher temperatures and shown that although we could accelerate thiolate desorption and thus exchange, separated molecular domains still do not reflect equilibrium distributions and depend strongly on the processing conditions [12].

We have also acquired evidence using TOF-SIMS that for some mixed composition SAMs the distribution of neighbor molecules within the film are not random. This is a natural result of phase separation—molecules are more likely to be found near identical molecules than if they were mixed randomly (in which case the probabilities on all length scales would be given by the surface density of each molecule).

In this paper we discuss the preference of these similar alkanethiol self-assembled systems to phase segregate. The presence of these phase-separated domains indicates that the equilibrium structures of these film compositions are phase separated on some length scale.

2. Experimental section

Substrates for this study were prepared by evaporation of gold (99.999%) onto the surface of freshly cleaved mica which was preheated in a vacuum to ~ 340 °C [13]. The base pressure in the chamber during evaporation was $\leq 6 \times 10^{-7}$ Torr. After ~ 100 nm of gold was deposited, the substrate temperature was returned to < 40 °C while still under vacuum, then the chamber was back-filled with purified nitrogen, the substrates removed, and immersed immediately into ethanolic solutions of either $\text{CH}_3(\text{CH}_2)_{15}\text{SH}$, $\text{CH}_3\text{O}_2\text{C}(\text{CH}_2)_{15}\text{SH}$, $\text{HOCH}_2(\text{CH}_2)_{15}\text{SH}$,

$\text{NCCH}_2(\text{CH}_2)_{15}\text{SH}$, or a combination of two of these thiols at 1 nM total thiol concentration. In this study, pure solutions of each thiol and mixed solutions of pairs of thiols were examined. At these concentrations, the thiols are soluble in ethanol, and readily form homogeneous solutions. The substrates were immersed in the solutions for four days at room temperature, after which the samples were withdrawn, rinsed extensively in ethanol, and dried under a stream of nitrogen. Mica-supported samples were analyzed using STM. Companion samples prepared on gold films on native oxide-covered single crystal Si(100) wafers (as described elsewhere [14]) were characterized by x-ray photoelectron spectroscopy (XPS), ellipsometry, and infrared spectroscopy (IRS) to verify the quality, thickness and composition of the self-assembled films [2, 15]. Samples prepared on gold-coated Si wafers were also studied using TOF-SIMS in the static regime (low total ion dose). The imaging TOF-SIMS instrument has been described elsewhere [16]. These samples were analyzed immediately after removal from ethanol, rinsing, and drying. The monolayer films were observed to be stable in air for the duration of the experiments with no evidence for the formation of sulfonates or other degradation products as shown by XPS, IR, and SIMS.

The STM images were recorded in air using a microwave-frequency-compatible beetle-style STM [17]. All the samples were studied using DC tunneling current to control the tip-sample separation. All images were recorded at tunneling gap impedances that ensured a large tip-sample separation, $10^9 \Omega$ [18]†. All STM images were recorded in constant tunneling current mode and are presented unfiltered. The tunneling current was 2 nA with a tip bias voltage of -2 V. The STM piezoelectric scanner calibrations were performed by recording atomic resolution images of surfaces of known crystallography.

The mechanism that allows nominally insulating organic films to be imaged remains unclear. Dürig *et al* have conducted simultaneous STM and atomic force microscopy (AFM) experiments on SAMs of $\text{HO}(\text{CH}_2)_{16}\text{SH}$ on gold [19]. From these simultaneous measurements, they concluded that the pressure induced by the probe tip must play an important role in the ability of electrons to tunnel through these films. Other studies have shown how the presence of 'insulating' adsorbates assists in the tunneling of electrons in the STM tunnel junction without the need for compressing adsorbates [20].

We have previously shown how STM can be used to determine the distribution of mixed composition self-assembled films of *n*-alkanethiol molecules, $\text{CH}_3(\text{CH}_2)_{15}\text{SH}$ and $\text{CH}_3\text{O}_2\text{C}(\text{CH}_2)_{15}\text{SH}$, on Au{111} [7, 8]. After imaging single composition films and characterizing the features (such as point defects) found in STM images, we imaged mixed composition SAMs with 1:3, 1:1, and 3:1 ratios of the two thiols [7–9]. The most striking features were the presence of nanometer-scale domains that were differentiated in topographic images. The two molecular domains appeared at a height difference of 1 Å

† Since this work was done, it has been found that for SAMs of shorter chains ($\text{CH}_3(\text{CH}_2)_n\text{S}-$, where $n \lesssim 12$) at higher tunneling gap impedances ($R \gtrsim 10^{11} \Omega$), one can routinely obtain molecular resolution.

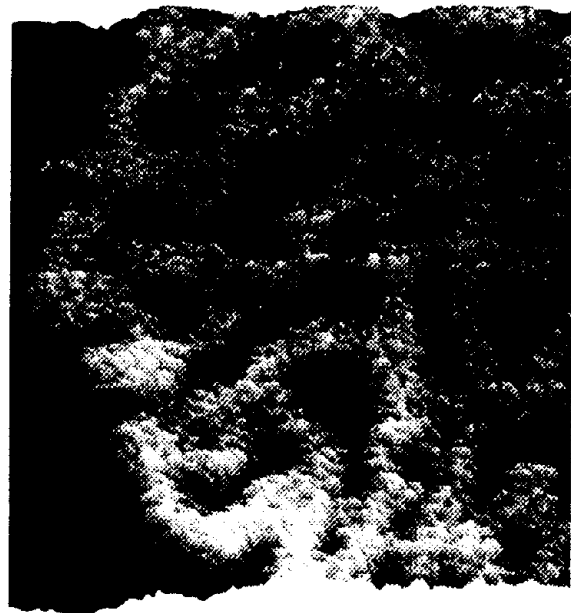


Figure 1. A STM image showing a $450 \times 450 \text{ \AA}$ area of a SAM of a 1:1 ratio of $\text{CH}_3\text{O}_2\text{C}(\text{CH}_2)_{15}\text{SH}$ and $\text{CH}_3(\text{CH}_2)_{15}\text{SH}$ on Au(111). The image was recorded in constant current mode at a tunneling current of 2 nA and a tip bias voltage of -2 V . The vertical scale shows a 3 \AA range in topography. On the left side of the image is a monatomic height step in the Au substrate. The image is shown unfiltered.

in constant current images at 10^9 \Omega gap impedance. In each case, the ratio of the areas of the domains was found to be equal to the ratio of the two thiols in the deposition solutions. Based on the analysis of the areas and the strong correlation with the expected surface concentrations, we assigned these topographic features as domains of the two thiolate species in the films.

3. Results

Figure 1 shows a STM image of a $450 \text{ \AA} \times 450 \text{ \AA}$ region of a SAM of a 1:1 ratio of $\text{CH}_3\text{O}_2\text{C}(\text{CH}_2)_{15}\text{SH}$ and $\text{CH}_3(\text{CH}_2)_{15}\text{SH}$ on Au. The phase-separated domains appear as regions with a 1 \AA difference in height from the neighboring domains of the other thiolate moiety. From our previous studies of various composition ratios [7, 8], we are able to assign the higher of the two domains to the methyl-ester-terminated molecule. These domains are highly intertwined which results in them being long and relatively narrow. This is discussed further in section 4 below.

As seen in the STM images, the distribution of molecules on the surface is clearly not random and thus should be evident in surface spectroscopies. To this end, we have explored the nanometer length scale distributions by TOF-SIMS. The spot size of the ion beam used for imaging currently has a lower limit of $\sim 500 \text{ \AA}$ [16], too large to identify phase-separated domains of the size shown in figure 1. Indeed, no phase separation in these films is observed by direct TOF-SIMS imaging. Instead, we use the propensity of nearby adsorbed molecules to

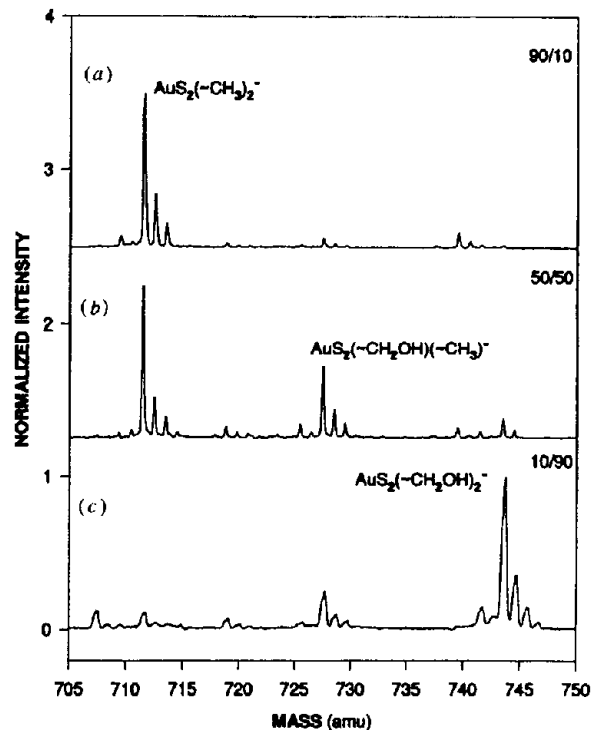


Figure 2. Secondary ion mass spectra of mixed composition SAMs of $\text{CH}_3(\text{CH}_2)_{15}\text{SH}$ and $\text{HO-CH}_2(\text{CH}_2)_{15}\text{SH}$ on Au for nominal mixtures of: (a) 9:1, (b) 1:1, and (c) 1:9. The region shown once again includes the ions composed of two thiolates and one Au atom. The suppressed peak intensity of the central set of peaks in (b) indicates that the thiolates are *not* randomly distributed within the film as described in the text. The spectra are offset for clarity.

be ejected simultaneously from the collision cascade due to single ion impacts. The higher effective 'resolution' in this case results from the localization of the collision cascade. Nearby adsorbates then are either desorbed bound together or recombine in the gas phase in the vicinity of the surface. Recent molecular dynamics simulations show that the lateral sensitivity in such a measurement is $\sim 20 \text{ \AA}$ [16]†.

Figure 2 shows the SIMS spectra for 9:1, 1:1, and 1:9 mixtures of $\text{CH}_3(\text{CH}_2)_{15}\text{SH}$ and $\text{HOCH}_2(\text{CH}_2)_{15}\text{SH}$ in the region where ions composed of two thiolate species bound to a single Au atom are found. Figure 3 shows the SIMS spectra for 9:1, 1:1, and 1:9 mixtures of $\text{HOCH}_2(\text{CH}_2)_{15}\text{SH}$, and $\text{NCCH}_2(\text{CH}_2)_{15}\text{SH}$ in the equivalent spectral region. As noted above, we interpret the presence of these ions as being due predominantly to two thiolate species being simultaneously ejected during the same collision cascade from a single incident (Ga^+) ion. By analyzing the areas of the mixed thiolate ions—the central peaks in the spectra—we can determine the extent to which one thiolate is surrounded by a purely statistical distribution of each thiol or whether the surface is patterned on this $\sim 20 \text{ \AA}$ length scale.

† While the area of damage from a single ion impact has a radius of $\sim 50 \text{ \AA}$, in molecular dynamics simulations such as those described in [16], the directions of the ejected particles from a single ion impact are such that only particles ejected within $\sim 20 \text{ \AA}$ are likely to recombine.

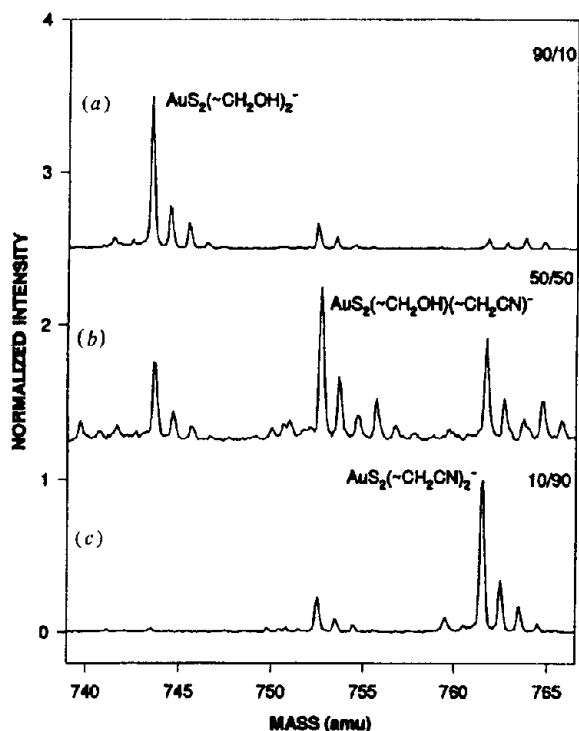


Figure 3. Secondary ion mass spectra of mixed composition SAMs of HO-CH₂(CH₂)₁₅SH and NC-CH₂(CH₂)₁₅SH on Au for nominal mixtures of: (a) 9:1, (b) 1:1, and (c) 1:9. The region shown includes the ions composed of two thiolates and one Au atom. The peak intensities are in each case consistent with randomly distributed molecules within the film. The spectra are offset for clarity.

For this analysis, we first determine the expected spatial distribution of molecules given by a random filling of adsorbate sites in the lattice. Then, using this distribution, we determine the propensity for observing the various pairs by estimating the combined ejection, ionization, and detection probabilities. This is our detection efficiency for observing a particular molecular pair together in a cluster ion if the two molecules are within the area of effect of a single collision cascade. This step of determining the detection efficiency remains the weak link in our analysis. Finally, by comparing the observed mass spectra with those predicted for the randomly distributed molecules given our detection efficiency, we are able to determine the extent to which the molecules are separated on the surface. For STM images with molecular lattice resolution we are able to perform this same type of analysis where our 'detection efficiency' is essentially unity [18]†.

Analysis of the SIMS data indicates that the mixtures shown in figure 2 are patterned (separated) whereas those shown in figure 3 appear to be consistent with a statistical distribution of thiolates. The integrated area of the mixed thiolate negative ion (CH₃(CH₂)₁₅S-Au⁻-S(CH₂)₁₅CH₂OH) for the 1:1 ratio film in figure 2 (spectrum *b*) is reduced by a factor of 1.6 from what would be found for a statistical distribution of molecules within the film, and is reduced by a factor as high as 4.9 for a

† This approach has been used for determining quantitatively the extent of separation effected by various processing conditions [12].

9:1 ratio film (spectrum *a*). By careful analysis of these integrated intensities we expect to be able to quantify the fraction of the surface covered by 'interface lines' versus the fraction covered by pure domains of one molecule. Within the errors inherent in our analysis, the SIMS data indicates that the mixtures shown in figure 3 appear to be consistent with randomly distributed molecules.

Mixed composition SAMs show greatly reduced defect densities compared with the single composition films that we have studied prepared under identical deposition conditions [7]. We have tentatively assigned this to the interface tension that is a consequence of the differing intermolecular interactions. Thus, a quantitative measurement of the fraction of the surface covered by an interface would be an important parameter in the preparation of nearly ideal films. We have shown elsewhere how these defects play a critical role in controlling film structure, and in allowing the exchange and the insertion of molecules into these films [12, 21].

4. Discussion

We have previously shown how molecules exchanging between domains within the film can account for some portion of domain formation and growth [7]. The observed time scale of this exchange is quite slow (about 1 exchange per site per hour), but the actual growth rate is most likely to be faster. This is explained by the initial stages of the two-dimensional domain growth being at or along the interfaces which is much more rapid than the latter part of the growth. Consider an initially random mixture within the film with the cross-interaction between adsorbates A and B lower than that of either like intermolecular attraction A-A or B-B. Such a system starts out in a high energy configuration because it has a high total interface length and thus a large contribution from the many A-B interactions. It then evolves to lower energy configurations (towards thermodynamic equilibrium), by reducing the interface length and thus interface energy through the growth of increasingly larger domains. Finally, the system moves relatively slowly through its final 'annealing' stage where smaller domains merge to form larger ones. This consumption of smaller domains results in a reduction of the overall interfacial energy and has been observed in time lapse STM imaging [7]. We have observed the reduction of domain curvature by molecular exchange between domains. These observations lend support to the interfacial energy reduction argument presented above.

In the 1:1 samples we see that in STM images the domains are highly connected, but relatively narrow. In the 1:3 methyl-terminated to methyl-ester-terminated samples the methyl-ester-terminated domains are also extended and nearly continuous. In the complementary 3:1 mixture, the majority methyl-terminated phase shows no apparent propensity to form extended domains. These observations allow us to rank the relative strengths of the sampled interactions. The cross-interaction between methyl-terminated molecules and methyl-ester-terminated molecules is lower than either of the like molecule attractions. Further, the methyl-ester-to-methyl-ester

intermolecular attraction is stronger than that for the methyl-terminated molecules.

While the imaging scale of the SIMS instrument is too coarse to observe the domains of phase-segregated molecules, the much finer scale due to the collision cascade can be used to determine the extent to which adsorbates are separated. This requires a careful calibration or a detailed understanding of the detection efficiency of cluster ions [22]. Once the details of the interface regions are understood on the molecular scale, it may be possible to use macroscopically patterned films such as those formed by microcontact printing [23] for calibration of the detection efficiency of molecular pairs.

5. Conclusions and future prospects

The techniques of STM and SIMS have allowed us to probe the nanometer-scale structure and stability of mixed composition SAMs of *n*-alkanethiols on Au{111}. Using these binary films, we have shown that mixed composition SAMs of even very similar alkanethiols on Au{111} phase separate into nanometer-scale domains of each component. These observations aid in the development of a fundamental understanding of the formation of nanometer-scale domains and in the application of mixed composition SAMs to the generation and stabilization of spatial patterns of adsorbed molecules. We note that these naturally formed patterns and structures can be used as a basis for further creation of nanometer-scale structures [24].

We are currently attempting to create varying nanometer-scale surface structures by changing our deposition strategies and by post-deposition modification of the terminal functional groups exposed on the SAM. We are continuing our efforts to measure quantitatively the surface interface density using SIMS.

Acknowledgments

The authors would like to thank Lloyd Bumm, Michael Cygan, Doug Doren, Barbara Garrison, Sanat Kumar, Ernst Meyer, Bruno Michel, and John Vickerman for helpful discussions and Kyle Krom for help in the preparation of the figures. The authors gratefully acknowledge the National Science Foundation Chemistry, Graduate Research Traineeship Materials Research, and Presidential Young Investigator Programs, the National Institutes of Health, the Office of Naval Research, the Alfred P Sloan Foundation (PSW), the Biotechnology Research and Development Corporation, and the Shell Foundation for supporting this research.

References

- [1] Dubois L H and Nuzzo R G 1992 *Ann. Rev. Phys. Chem.* **43** 437 and references therein
- [2] Nuzzo R G, Dubois L H and Allara D L 1990 *J. Am. Chem. Soc.* **112** 558
- [3] Von Tscharner V and McConnell H M 1981 *Biophys. J.* **36** 409
Heckl W M and Möhwald H 1986 *Ber. Bunsenges. Phys. Chem.* **90** 3249

- [4] Overney R M, Meyer E, Frommer J, Brodbeck D, Lüthi R, Howald L, Güntherodt H-J, Fujihara M, Takano H and Gotoh Y 1992 *Nature* **359** 133
Frommer J, Lüthi R, Meyer E, Anselmetti D, Dreier M, Overney R, Güntherodt H-J and Fujihara M 1993 *Nature* **364** 198
- [5] Meyer E, Overney R, Lüthi R, Brodbeck D, Howald L, Frommer J, Güntherodt H-J, Wolter O, Fujihara M, Takano H and Gotoh Y 1992 *Thin Solid Films* **220** 132
- [6] Frisbie C D, Rozsnyai L F, Noy A, Wrighton M S and Lieber C M 1994 *Science* **265** 2071
- [7] Stranick S J, Parikh A N, Tao Y-T, Allara D L and Weiss P S 1994 *J. Phys. Chem.* **98** 7636
- [8] Stranick S J, Kamna M M, Krom K R, Parikh A N, Allara D L and Weiss P S 1994 *J. Vac. Sci. Technol. B* **12** 2004
- [9] Stranick S J, Parikh A N, Allara D L and Weiss P S 1994 *J. Phys. Chem.* **98** 11136
- [10] Folkers J P, Laibinis P E, Whitesides G M and Deutch J 1994 *J. Phys. Chem.* **98** 563
- [11] Collard D M and Fox M A 1991 *Langmuir* **7** 1192
Frisbie C D, Wollman E W, Martin J R and Wrighton M S 1993 *J. Vac. Sci. Technol. A* **11** 2368
Wood M C, Atre S V, Winograd N, Liedberg B and Allara D L to be published
- [12] Bumm L A, Arnold J J, Charles L F, Cygan M T, Dunbar T D, Allara D L and Weiss P S to be published
- [13] Chidsey C E D, Loiacono D N, Sleater T and Nakahara S 1988 *Surf. Sci.* **20** 45
Hallmark V M, Chiang S, Rabolt J F, Swalen J D and Wilson R J 1987 *Phys. Rev. Lett.* **59** 2879
Widrig C A, Alves C A and Porter M D 1991 *J. Am. Chem. Soc.* **113** 2805
- [14] Nuzzo R G, Fusco F A and Allara D L 1987 *J. Am. Chem. Soc.* **109** 2358
Troughton E B, Bain C D, Whitesides G M, Nuzzo R G, Allara D L and Porter M D 1988 *Langmuir* **4** 365
- [15] Laibinis P E, Whitesides G M, Allara D L, Tao Y-T, Parikh A N and Nuzzo R G 1991 *J. Am. Chem. Soc.* **113** 7152
- [16] Winograd N 1993 *Anal. Chem.* **65** 622A
- [17] Besocke K 1987 *Surf. Sci.* **181** 145
Frohn J, Wolf J F, Besocke K and Teske M 1989 *Rev. Sci. Instrum.* **60** 1200
Stranick S J and Weiss P S 1994 *Rev. Sci. Instrum.* **65** 918
- [18] Schonenberger C, Sondag-Huethorst J A M, Jorritsma J and Fokink L G J 1994 *Langmuir* **10** 4103
Poirier G E and Pylant E D 1996 *Science* **272** 1145
Bumm L A, Arnold J J, Cygan M T, Dunbar T D, Burgin T P, Jones II L, Allara D L, Tour J M and Weiss P S 1996 *Science* **271** 1705
- [19] Dürig U, Züger O, Michel B, Häussling L and Ringsdorf H 1993 *Phys. Rev. B* **48** 1711
- [20] Eigler D M, Weiss P S, Schweizer E K and Lang N D 1991 *Phys. Rev. Lett.* **66** 1189
Weiss P S and Eigler D M 1993 *Phys. Rev. Lett.* **71** 3139
Weiss P S 1994 *Trends Anal. Chem.* **13** 61
- [21] Bumm L A, Arnold J J, Cygan M T, Dunbar T D, Burgin T P, Jones II L, Allara D L, Tour J M and Weiss P S 1996 *Science* **271** 1705
- [22] Wood M C 1995 *PhD Thesis* The Pennsylvania State University
- [23] Wilbur J L, Kumar A, Kim E and Whitesides G M 1994 *Adv. Mater.* **6** 600
Xia Y, Mrksich M, Kim E and Whitesides G M 1995 *J. Am. Chem. Soc.* **117** 9576
Wilbur J M, Kumar A, Biebuyk H A, Kim E and Whitesides G M 1996 *Nanotechnology* **7** 452
- [24] Stranick S J, Kamna M M and Weiss P S 1996 *Nanotechnology* **7** 443